

Rotational dynamics of neutral O_2 driven by linearly, elliptically and circularly polarized femtosecond pulsed lasers

Ting Xu(许婷), Jin-Peng Ma(马金鹏), Xiao-Qing Hu(胡晓青), Yin-Song Tang(唐寅淞), Si-Qi Pei(裴思琪), Cong-Cong Jia(贾聪聪), Yong-Wu(吴勇), and Jian-Guo Wang(王建国)
Citation: Chin. Phys. B, 2025, 34 (**5**): 053301. DOI: 10.1088/1674-1056/adbeea
http://cpb.iphy.ac.cn; http://iopscience.iop.org/cpb

What follows is a list of articles you may be interested in

Optical spectroscopy of CrO and electronic states of the Cr group metal monoxides

Lei Zhang(张磊), Yao Yu(于尧), Xinwen Ma(马新文), and Jie Yang(杨杰)
Chin. Phys. B, 2023, 32 (**5**): 053301. DOI: 10.1088/1674-1056/acb763

Line positions, intensities, and Einstein *A* coefficients for 3-0 band of $^{12}C^{16}O$: A spectroscopy learning method

Zhi-Xiang Fan(范志祥), Zhi-Zhang Ni(倪志樟), Jie-Jie He(贺洁洁), Yi-Fan Wang(王一凡), Qun-Chao Fan(樊群超), Jia Fu(付佳), Yong-Gen Xu(徐勇根), Hui-Dong Li(李会东), Jie Ma(马杰), and Feng Xie(谢锋)
Chin. Phys. B, 2021, 30 (**12**): 123301. DOI: 10.1088/1674-1056/ac3069

Tracking coherent low frequency vibrational information of Rh101 in ground and excited electronic states by broadband transient grating spectroscopy

Wei Zhang(张伟), Xiao-Song Liu(刘小嵩), Zan-Hao Wang(王赞浩), Yun-Fei Song(宋云飞), Yan-Qiang Yang(杨延强)
Chin. Phys. B, 2018, 27 (**12**): 123301. DOI: 10.1088/1674-1056/27/12/123301

Photoassociation spectra of ultracold $^{85}Rb_2$ molecule in 0_u^+ long range state near the $5S_{1/2}+5P_{1/2}$ asymptote

Guodong Zhao(赵国栋), Dianqiang Su(苏殿强), Zhonghua Ji(姬中华), Tengfei Meng(孟腾飞), Yanting Zhao(赵延霆), Liantuan Xiao(肖连团), Suotang Jia(贾锁堂)
Chin. Phys. B, 2017, 26 (**8**): 083301. DOI: 10.1088/1674-1056/26/8/083301

Infrared diode laser spectroscopy of O_2–N_2O van der Waals complex in the ν_1 symmetric stretch region of N_2O

Li Song (李松), Zheng Rui (郑锐), Duan Chuan-Xi (段传喜)
Chin. Phys. B, 2014, 23 (**12**): 123301. DOI: 10.1088/1674-1056/23/12/123301

Rotational dynamics of neutral O_2 driven by linearly, elliptically and circularly polarized femtosecond pulsed lasers

Ting Xu(许婷), Jin-Peng Ma(马金鹏), Xiao-Qing Hu(胡晓青)†, Yin-Song Tang(唐寅淞), Si-Qi Pei(裴思琪), Cong-Cong Jia(贾聪聪), Yong-Wu(吴勇), and Jian-Guo Wang(王建国)

National Key Laboratory of Computational Physics, Institute of Applied Physics and Computational Mathematics, Beijing 100088, *China*

(Received 13 February 2025; revised manuscript received 9 March 2025; accepted manuscript online 11 March 2025)

Rotational dynamics simulations of neutral O_2 molecules driven by linearly, elliptically and circularly polarized femtosecond pulsed lasers are carried out using a full quantum time-dependent wave packet evolution method. Here, the direction of laser propagation is set along the z axis, and the polarization plane is restricted to the xy plane. The results indicate that the alignment of O_2 molecules in the z direction is weakly affected by varying the ellipticity when the total laser intensity is held constant. For rotation within the xy plane, the linearly polarized laser significantly excites rotational motion, with the degree of excitation increasing as the ellipticity increases. In contrast, under the influence of a circularly polarized laser, the angular distribution of O_2 molecules in the xy plane remains isotropic. Additionally, the effects of the initial rotational quantum number, the temperature of the O_2 molecules and the nuclear spin on laser-induced alignment are discussed.

Keywords: rotational dynamic, laser alignment, time-dependent wave packet simulation

PACS: 33.15.Mt, 33.20.Sn, 33.20.Wr

DOI: 10.1088/1674-1056/adbeea **CSTR:** 32038.14.CPB.adbeea

1. Introduction

Rotation, as one of the most sensitive modes of molecular motion, can be easily excited even by long-range and weak interactions, significantly influencing the dynamical processes of molecules and their ions.[1–8] For example, at low temperatures the weak van der Waals interaction between neutral atoms and molecules can exceed the molecular rotational energy. This, in turn, restricts molecular rotation and results in the formation of stable molecular clusters.[9] Additionally, the long-range Coulomb interaction between atomic and molecular ions can cause molecular fragments to rotate rapidly,[10] with rotation periods being reduced to the order of 100 fs. Even in the case of ultrafast electron/heavy ion–molecule collisions[11–13] that occur on attosecond time scales, molecular rotational states can be excited due to the anisotropy of the molecular electron density distribution. Comprehending and controlling the rotational behavior of molecules and their ions is of particular significance for the study of molecular structure and reaction dynamics.[14,15]

In recent decades, the use of femtosecond pulsed laser fields to manipulate the rotational behavior of polyatomic molecules has been widely applied in the study of laser-induced ultrafast dynamics of molecules and their ions.[16–21] Under the dipole approximation, the interaction between the laser and molecules can be expressed as $\boldsymbol{E}\cdot\boldsymbol{D}\cos\theta$, where θ is the angle between the laser field $\boldsymbol{E}$ and the molecular dipole moment $\boldsymbol{D}$. This interaction is directly related to the molecular orientation and leads to the excitation of rotational states in any dynamic process involving lasers. Ultimately, the coherent evolution of multiple rotational states results in the molecular orientation exhibiting periodic changes even after the laser field has ceased, a phenomenon known as molecular alignment.[22–27]

Recently, Guo *et al.*[28] reported the observation of Coriolis coupling, which is an interaction between nuclear rotational angular momentum and electronic axial angular momentum, during laser-induced molecular fragmentation. They traced the electronic structure of a dissociating O_2^+ molecule using a time-resolved Coulomb explosion imaging method with circularly polarized pump and linearly polarized probe laser pulses. Their research shows that the rotation–electron coupling facilitates a transition from the $1^4\Sigma_u^+$ electronic state to the neighboring $a^4\Pi_u$ electronic state of the O_2^+ molecule. Importantly, the duration of this transition is dictated by the rotational quantum number excited by the circularly polarized pump laser pulses, underscoring the significant role of rotational excitation in neutral molecules.

In this paper, we perform a full quantum time-dependent wave packet simulation[29,30] of the laser-induced rotational dynamics of O_2 based on the interaction picture. In our simulation, the standard non-resonant Raman excitation[2] process is primarily considered. We systematically discuss the excitation of the rotational quantum number and the time-dependent evolution of the rotational wave function of O_2 molecules under different laser polarization conditions. The analysis fo-

†Corresponding author. E-mail: xiaoqing-hu@foxmail.com

© 2025 Chinese Physical Society and IOP Publishing Ltd. All rights, including for text and data mining, AI training, and similar technologies, are reserved.

cuses on molecular rotations both along the laser propagation direction and within the polarization plane as laser parameters vary. Our simulations indicate that the rotation along the direction of laser propagation is mainly associated with the laser intensity and has a weaker dependence on ellipticity. In contrast, the rotation within the polarization plane can be modulated by the ellipticity of the laser.

This paper is organized as follows. In Section 2, we briefly discuss the theoretical model of the quantum time-dependent wave packet evolution method for O_2. Subsequently, in Section 3, we present the numerical results and discussion concerning molecular rotations in the laser propagation direction and polarization plane. Finally, in Section 4, our conclusions are given.

2. Numerical theory

In this work, we employ a full quantum time-dependent wave packet evolution method to simulate the rotational dynamics of neutral ground O_2 molecules. Here, our primary focus is on the standard non-resonant Raman excitation of the rotational states, which is triggered by the dipole polarization interaction between the laser and the molecules. For this simulation, the Hamiltonian of the system is formulated as

$$H = [H_{\rm a}(R, r_{\rm e}) + R_{\rm e}(R)] + P = H_0 + H', \tag{1}$$

where $H_{\rm a}$ is the adiabatic Hamiltonian, which includes the electronic and nuclear kinetic energy as well as the electron–electron and electron–nuclear potential energy. $R_{\rm e}$ is the rotational energy of O_2, which can be written as $R_{\rm e} = \frac{j(j+1)}{2\mu R^2}$, where μ is the molecular reduced mass and j is the rotational angular momentum. Considering that the oxygen nucleus is bosonic, the spatial wave function of the O_2 molecule must be symmetric. Therefore, for neutral O_2, the rotational quantum number j must be odd. The eigenstates of H_0 can be expressed as the product of vibrational and rotational wave functions, $\psi(R)Y_{j,m}(\theta,\phi)$. Here, the coupling between rotation and vibration is neglected because the vibration of the ground state O_2 molecule is scarcely excited, and only the ground electronic and vibrational state is considered in the calculations. θ is the angle between the O–O bond and the direction of laser propagation (the z-axis), and ϕ is the angle between the O–O bond and the positive x-axis. The polarization interaction P between the laser and O_2 molecule can be given as $-\boldsymbol{E}(t)^2(\alpha_{\parallel} \times \cos^2\gamma + \alpha_{\perp} \times \sin^2\gamma)$, where γ is the angle between the laser field and the O–O bond, and $\alpha_{\parallel}$ and $\alpha_{\perp}$ represent the parallel and perpendicular components of the dipole polarizability tensor, respectively. The electric field $\boldsymbol{E}(t)$ is given by $\boldsymbol{E}(t) = f(t)[E_x\hat{\boldsymbol{e}}_x \sin(\omega t) + E_y\hat{\boldsymbol{e}}_y \sin(\omega t + \pi/2)]$, where $f(t)$ is the envelope function of the laser pulse, expressed as $f(t) = \sin^2(\pi t/t_0)$ for $0 < t < t_0$. Here, E_0, ω and t_0 denote the peak amplitude of the electronic field, the carrier frequency and the pulse duration, respectively.

To solve the time-dependent Schrödinger equation (TDSE), we postulate that the wave function of the system at time t can be written as

$$\Psi(R,\theta,\phi,t) = \sum_{j,m} c_{j,m}(t)\psi(R)Y_{j,m}(\theta,\phi). \tag{2}$$

Based on Eq. (1), the solution to the TDSE at time $t + {\rm d}t$ can be expressed as follows:

$$\Psi(R,\theta,\phi,t+{\rm d}t) = {\rm e}^{-\frac{\rm i}{\hbar}H\,{\rm d}t}\Psi(R,\theta,\phi,t). \tag{3}$$

Using the second-order split operator method and Taylor expansion, we obtain

$$\begin{aligned} &{\rm e}^{-\frac{\rm i}{\hbar}H\,{\rm d}t} = {\rm e}^{-\frac{\rm i}{2\hbar}H_0\,{\rm d}t}\,{\rm e}^{-\frac{\rm i}{\hbar}H'\,{\rm d}t}\,{\rm e}^{-\frac{\rm i}{2\hbar}H_0\,{\rm d}t}, \\ &{\rm e}^{-\frac{\rm i}{\hbar}H'\,{\rm d}t} \simeq 1 - \frac{{\rm i}\,{\rm d}t}{\hbar}H' - \frac{{\rm d}t^2}{2\hbar^2}H'^2 + \frac{{\rm i}\,{\rm d}t^3}{6\hbar^3}H'^3. \end{aligned} \tag{4}$$

Finally, after determining the matrix elements of H', H'^2 and H'^3 in the space spanned by $\psi(R)Y_{j,m}(\theta,\phi)$, we can conduct the time-dependent evolution of the rotational wave function of the neutral ground state O_2.

3. Results and discussion

In this work, the femtosecond pulsed laser-induced rotational dynamics of neutral ground state O_2 are simulated using the full quantum time-dependent wave packet evolution method. The time-dependent rotational quantum numbers and wave function are obtained and illustrated in Figs. 1–4. Two linearly polarized lasers with a wavelength of 800 nm and a fixed phase difference of $\pi/2$ are employed to generate elliptically and circularly polarized lasers. Their intensities are denoted by I_x and I_y, and the total laser intensity is set to $I_x + I_y = 50$ TW/cm^2. The pulse duration t_0 is approximately 70 fs. In the current simulations, we investigate the rotational dynamics of O_2 molecules under four distinct laser conditions with different ellipticities: (0 TW/cm^2, 50 TW/cm^2), (10 TW/cm^2, 40 TW/cm^2), (20 TW/cm^2, 30 TW/cm^2) and (25 TW/cm^2, 25 TW/cm^2).

Figure 1 shows the simulated time-dependent rotational quantum numbers of O_2 with the initial rotational state of $Y_{1,0}(\theta,\phi)$. Since the polarization direction of the laser is set in the xy plane, the variation of the laser field is only related to ϕ and not to θ. The laser-induced non-resonant Raman excitation does not change the symmetry of the molecular rotational wave function in the θ dimension, that is, $\Delta j = 0, \pm 2$ and $\Delta m = 0, \pm 2$. As shown in Fig. 1(a), the molecular rotational quantum numbers are mainly excited from (1,0) to (3, $0/\pm 2$), and the populations of these three states are quite close to one another. As I_x increases, the populations of $(3, -2)$ and (3, 2) decrease significantly. When $I_x = I_y = 25$ TW/cm^2, the laser field can be approximated as isotropic in the xy plane, which results in $\Delta m = 0$.

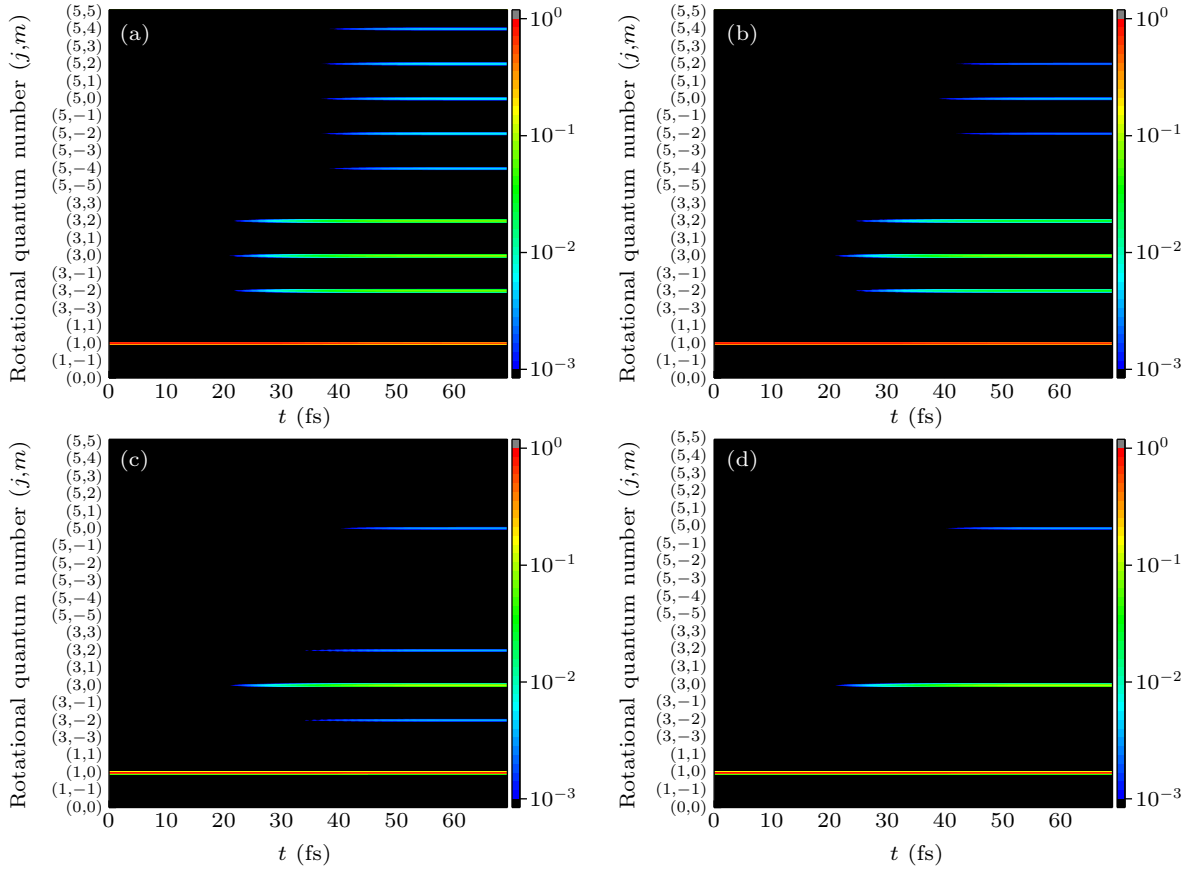


Fig. 1. Time-dependent rotational quantum numbers (j, m) for four laser parameter conditions with the same total laser intensity of 50 TW/cm^2 and the initial rotational state (1, 0): (a) linearly polarized laser with $I_x = 0$ TW/cm^2 and $I_y = 50$ TW/cm^2; (b) elliptically polarized laser with $I_x = 10$ TW/cm^2 and $I_y = 40$ TW/cm^2; (c) elliptically polarized laser with $I_x = 20$ TW/cm^2 and $I_y = 30$ TW/cm^2; (d) circularly polarized laser with $I_x = 25$ TW/cm^2 and $I_y = 25$ TW/cm^2.

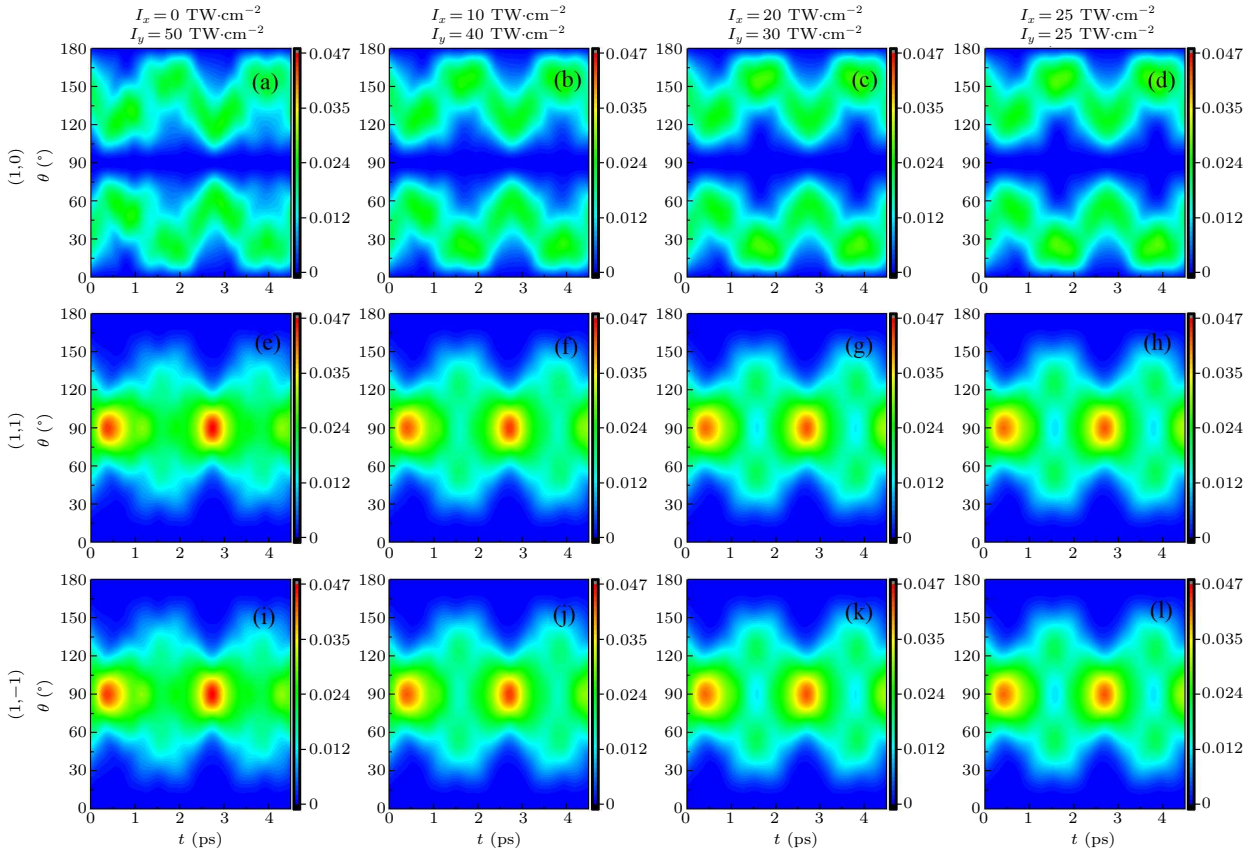


Fig. 2. The time-dependent distribution of θ for four laser parameter conditions and three different initial rotational states: $(1,0)$, $(1,1)$ and $(1,-1)$.

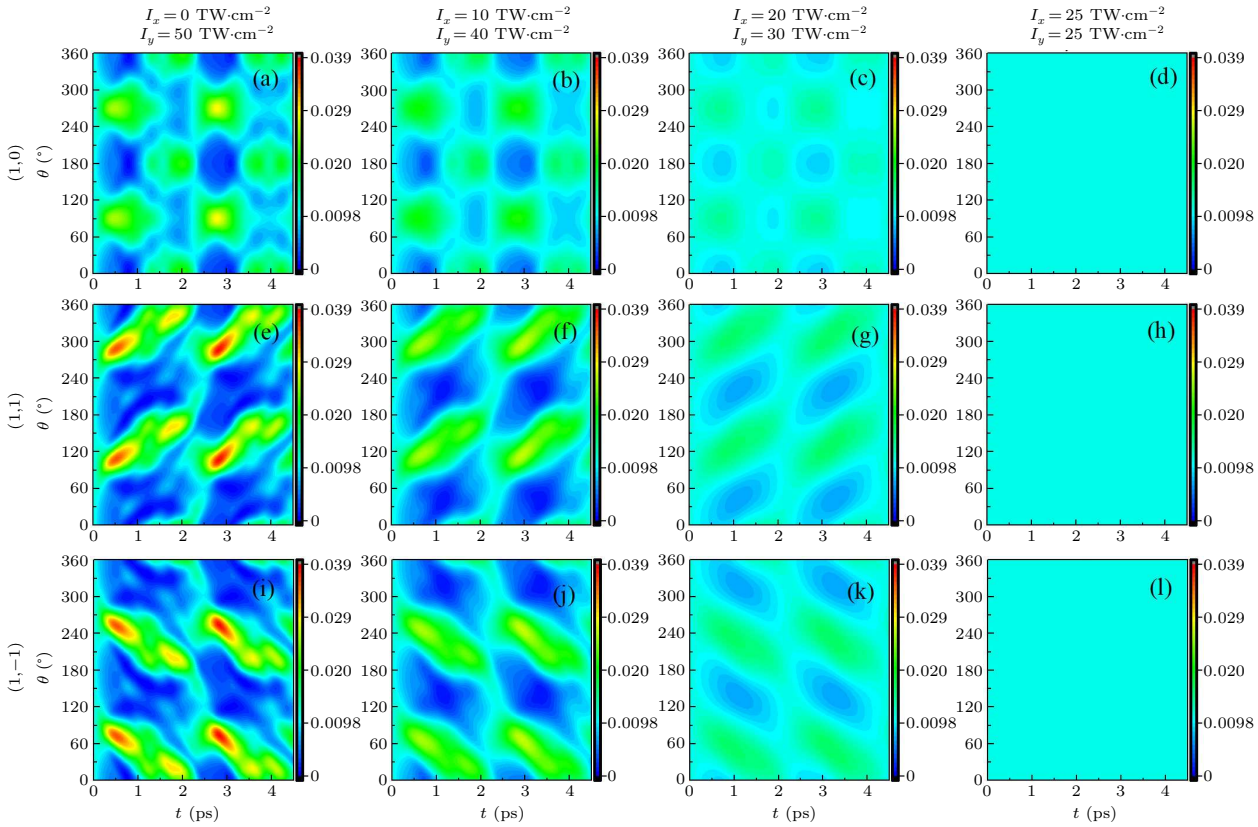


Fig. 3. Same as Fig. 2 except that the angular distribution is for ϕ.

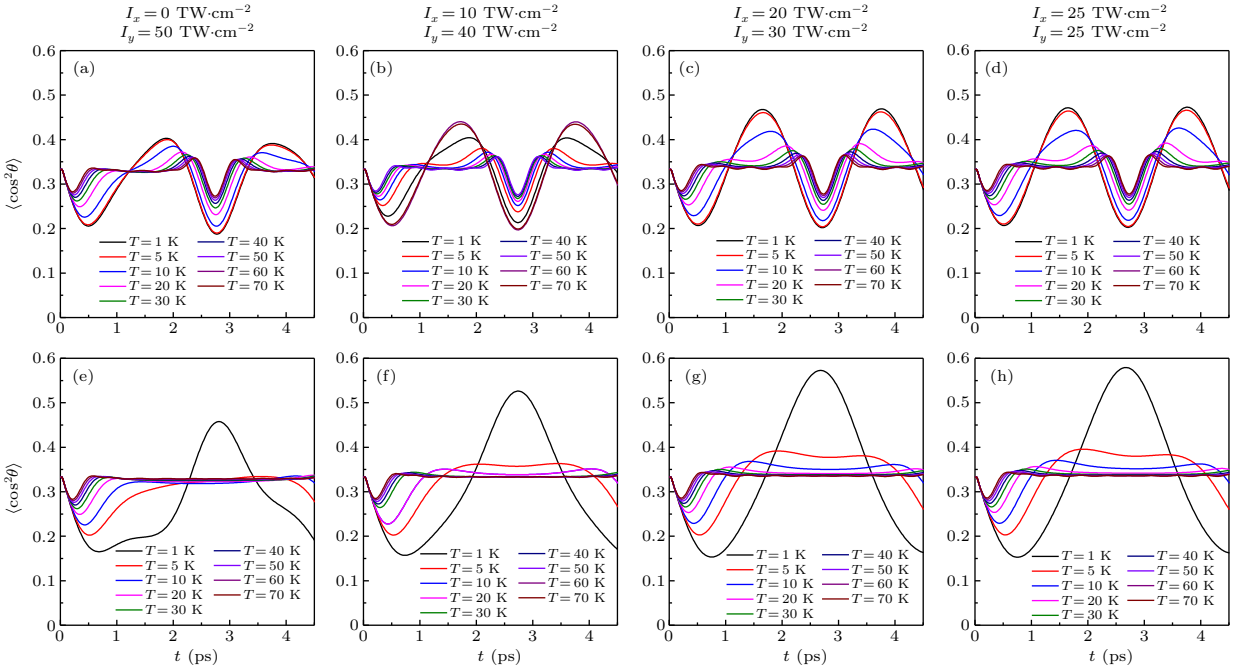


Fig. 4. The time-dependent alignment parameter $\langle\cos^2\theta\rangle$ with four laser parameter conditions at different temperatures (1–70 K): (a)–(d) for the results with the influence of nuclear spin and (e)–(h) for those without the influence of nuclear spin.

When comparing the calculated time-dependent rotational wave functions as a function of θ, a distinct cyclical rotation is observable in all the results shown in Fig. 2. This phenomenon is attributed to the coherent evolution of different rotational states, with the primary rotational period being determined by the energy difference between $j = 1$ and $j = 3$. Owing to the extremely low population of the state with $j = 5$, its contribution to the cyclical rotation is largely negligible. For the results induced by linearly, elliptically and circularly polarized lasers, the rotation in the θ direction remains essentially consistent. The minor differences come from the different populations of the excited rotational magnetic quantum

number m. Specifically, for the initial rotational state (1, 0), the initial orientation distribution of the molecule is concentrated along the z direction, which gives rise to a significant cyclical rotation towards the xy plane. On the contrary, for the results with the initial rotational states (1, 1) and (1, −1), the initial wave packet is already distributed around the xy plane. As a result, the laser can only drive the molecule to contract and expand within a small range around $\theta = 90°$. Moreover, the sign of the m quantum number has no impact on the rotation of the O_2 molecule in the θ dimension.

Figure 3 exhibits the simulated time-dependent rotational wave function as a function of ϕ. Unlike the rotation in the θ dimension, the rotation in the xy plane is affected not only by the ellipticity but also by the sign of the initial quantum number m. In Fig. 3(a), it can be seen that the initially isotropic molecules first transform towards the y-axis ($\phi = 90°/270°$), and subsequently rotate towards the x-axis ($\phi = 0°/180°/360°$). For the results corresponding to the initial rotational state (1, 1) in Fig. 3(e) and (1, −1) in Fig. 3(i), a similar cyclical rotational is observable. However, the rotation for (1, 1) is a clockwise rotation, while that for (1, −1) is counterclockwise. As anticipated, this rotation gradually weakens as I_x increases.

In Fig. 4, we discuss the effects of temperature and nuclear spin on laser-induced alignment. According to the Boltzmann distribution, the populations of the initial rotational quantum numbers of the O_2 molecule can be theoretically calculated. Since the oxygen nucleus is a boson, the spatial wave function of the O_2 molecule must be symmetric, and the rotational quantum number j must be odd for neutral O_2. Therefore, the lowest rotational state of O_2 is $j = 1$. With an increase in temperature, the initial rotational state can populate higher levels, such as $j = 3$, $j = 5$ and so on. However, these states are difficult to excite further due to the weak laser field with a total intensity of 50 TW/cm^2. Consequently, the periodic changes in angular distribution are caused by the coherent evolution of rotational states, which involves the excitation of ground state molecules with $j = 1$ and the de-excitation of O_2 molecules with $j = 3$. Thus, even when the initial temperature rises to 70 K, the cyclical rotation dominated by the coherent evolution of $j = 1$ and $j = 3$ can still be easily identified, and the O_2 molecule achieves a good alignment effect after 2.77 ps, as shown in Figs. 4(a)–4(d).

Quantitatively, for the results of the linearly polarized laser at 1 K shown in Fig. 4(a), the minimum and maximum values of the alignment parameter $\langle\cos^2\theta\rangle$ are about 0.19 in 2.77 ps and 0.40 in 1.88 ps, respectively. With the temperature increased to 70 K, the minimum value of the alignment parameter $\langle\cos^2\theta\rangle$ can reach 0.27, which indicates that the rotational wave packets of O_2 molecules are populated around the xy plane. By comparing the results in Figs. 4(a)–4(d), we can conclude that the influence of ellipticity on laser alignment is independent of temperature. If we disregard the nuclear spin of the oxygen atom and assume that the molecular rotational state can occupy any state, then as the temperature increases the molecular rotational quantum number will be populated to $j = 0, 1, 2, 3, \ldots$. The easiest transition channel becomes $j = 0 \leftrightarrow 2$, while transitions $j = 1 \leftrightarrow 3$ and $j = 2 \leftrightarrow 4$ also contribute to the result, and their effects increase rapidly as the temperature rises. Even when the molecular temperature is 10 K, there will still be multiple rotation modes occurring simultaneously, resulting in the disappearance of cyclical rotation. Finally, the laser will not be able to align O_2 molecules without the effect of nuclear spin at temperatures above 10 K.

4. Conclusion

In summary, the rotational dynamics simulations of neutral O_2 molecules driven by linearly, elliptically and circularly polarized femtosecond pulsed lasers are performed using a full quantum time-dependent wave packet evolution method. The simulated results indicate that all types of femtosecond pulsed lasers — linear, elliptical and circular — can align the molecular orientation along the propagation direction. Notably, the degree of alignment does not show an obvious dependence on the ellipticity; instead, it depends solely on the total laser intensity. Further, changing the ellipticity of the laser will control the rotation of the molecules within the polarization plane until the laser becomes circularly polarized, and the cyclical rotation of the polarization plane will disappear. Our results also show that due to the fact that the rotational quantum number of the neutral ground state O_2 molecule can only be odd, the main components of the initial molecular rotation states and the laser-induced rotational transitions change slowly with the increase in temperature. Therefore, when the initial temperature is increased to 70 K, the O_2 molecules can still achieve a good alignment effect after 2.77 ps. Our research is of great significance for the study of molecular orientation, rotational vibration coupling and rotational electron coupling dynamics.

Acknowledgments

Project supported by the National Key Research and Development Program of China (Grant No. 2022YFA1602502) and the National Natural Science Foundation of China (Grant No. 12450404).

References

[1] Rosca-Pruna F and Vrakking M J J 2001 *Phys. Rev. Lett.* **87** 153902
[2] Stapelfeldt H and Seideman T 2003 *Rev. Mod. Phys.* **75** 543
[3] Spanner M, Shapiro E A, and Ivanov M 2004 *Phys. Rev. Lett.* **92** 093001
[4] Ramakrishna S and Seideman T 2007 *Phys. Rev. Lett.* **99** 103001
[5] Anis F and Esry B D 2008 *Phys. Rev. A* **77** 033416
[6] Vozzi C, Negro M, Calegari F, Sansone G, Nisoli M, Silvestri S De, and Stagira S 2011 *Phys. Rev. A* **77** 033416

[7] Sondergaard A A, Zillich R E and Stapelfeldt H 2017 *J. Chem. Phys.* **147** 074304
[8] Koch C P, Lemeshko M and Sugny D 2019 *Rev. Mod. Phys.* **91** 035005
[9] Patel K, Butler P R, Ellis A M and Wheeler M D 2003 *J. Chem. Phys.* **119** 909
[10] Zhu X L, Hu X Q, Yan S C, Peng Y G, Feng W T, Guo D L, Gao Y, Zhang S F, Cassimi A, Xu J W, Zhao D M, Dong D P, Hai B, Wu Y, Wang J G and Ma X W 2020 *Nat. Commun.* **11** 2987
[11] Rohmund F, Campbell E E B, Knospe O, Seifert G and Schmidt R 1996 *Phys. Rev. Lett.* **76** 3289
[12] Sakimoto K 2004 *Phys. Rev. A* **69** 042710
[13] Liu Y Z and Zahed I 2018 *Phys. Rev. Lett.* **120** 032001
[14] Litvinyuk I V, Lee K F, Dooley P W, Rayner D M, Villeneuve D M and Corkum P B 2003 *Phys. Rev. Lett.* **90** 233003
[15] Hossain M M, Esaki N and Sakai H 2024 *Phys. Rev. A* **108** 063109
[16] Pitzer M, Kunitski M, Johnson A S, Jahnke T, Sann H, Sturm F, Schmidt L P H, Schmidt-Böcking H, Dörner R, Stohner J, Kiedrowski J, Reggelin M, Marquardt S, Schiesser A, Berger R and Schöffler M S 2013 *Science* **341** 1096
[17] Mizuse K, Kitano K, Hasegawa H and Ohshima Y 2015 *Sci. Adv.* **1** e1400185
[18] Lin K, Song Q Y, Gong X C, Ji Q Y, Pan H F, Ding J X, Zeng H P and Wu J 2015 *Phys. Rev. A* **92** 013410
[19] Kranabetter L, Kristensen H H, Ghazaryan A, Schouder C A, Chatterley A S, Janssen P, Jensen F, Zillich R E, Lemeshko M and Stapelfeldt H 2023 *Phys. Rev. Lett.* **131** 053201
[20] Bournazel M, Ma J, Billard F, Hertz E, Wu J, Boulet C, Hartmann J M and Faucher O 2023 *Phys. Rev. A* **107** 023115
[21] Lu C X, Xu L, Zhou L R, Shi M H, Lu P F, Li W X, Dörner R, Lin K and Wu J 2024 *Nat. Commun.* **15** 4360
[22] Seideman T 1995 *J. Chem. Phys.* **103** 7887
[23] Rosca-Pruna F and Vrakking M J J 2001 *Phys. Rev. Lett.* **87** 153902
[24] Dooley P W, Litvinyuk I V, Lee K F, Rayner D M, Spanner M, Villeneuve D M and Corkum P B 2003 *Phys. Rev. A* **68** 023406
[25] Chatterley A S, Shepperson B and Stapelfeldt H 2017 *Phys. Rev. Lett.* **119** 073202
[26] Trippel S, Wiese J, Mullins T and Küpper J 2018 *J. Chem. Phys.* **148** 101103
[27] Chatterley A S, Baatrup M O, Schouder C A and Stapelfeldt H 2020 *Phys. Chem. Chem. Phys.* **22** 3245
[28] Guo K Y, Hu X Q, Li M, Jia C C, Zhang S B, Cao C P, Xie W H, Cao W, Liu K L, Zhou Y M, Wu Y, Wang J G and Lu P X 2024 *Ultrafast Sci.* **4** 1
[29] Wang Z Z, Hu X Q, Xue X R, Zhou S P, Li X K, Yang Y Z, Zhou J Q, Shu Z, Zhao B C, Yu X T, Gong M M, Wang Z P, Ma P, Wu Y, Chen X J, Wang J G, Ren X G, Wang C C and Ding, D J 2023 *Nat. Commun.* **14** 5420
[30] Zhou J Q, Jia S K, Hu X Q, Wang E L, Xue X R, Wu Y, Wang J G, Dorn A and Ren X G 2023 *Phys. Rev. Lett.* **130** 233001